Journal of Fluorine Chemistry 130 (2009) 836–845

Contents lists available at ScienceDirect

Journal of Fluorine Chemistry

journal homepage: www.elsevier.com/locate/fluor

The structure and energetics of triplet [B, C, F, H_2]

Carol A. Deakyne [a,*], Haunani M. Thomas [a], Joel F. Liebman [b,**]

[a] Department of Chemistry, University of Missouri-Columbia, 601 S. College Avenue, Columbia, MO 65211-8600, USA
[b] Department of Chemistry and Biochemistry, University of Maryland, Baltimore County, 1000 Hilltop Circle, Baltimore, MD 21250, USA

ARTICLE INFO

Article history:
Received 23 May 2009
Received in revised form 9 July 2009
Accepted 9 July 2009
Available online 17 July 2009

This paper is dedicated to Henry Selig on the occasion of his winning the 2008 Award for Creative Work in Fluorine Chemistry given by the American Chemical Society.

Keywords:
Ab initio quantum chemical calculations
Boron–fluorine triplet compounds
Hydrogen bonding
Isoelectronic analogies
Multiple energy minima
Transition states
Enthalpies of formation
Bond dissociation energies

ABSTRACT

In the current paper, we discuss our high level quantum chemical results for the structure and energetics of triplet (and hence open-shell) isomers corresponding to the stoichiometry of one boron, carbon, and fluorine apiece, and two hydrogens. While partially bond-ruptured excited ketene- and diazomethane-like $H_2C^{\bullet}$–$B^{\bullet}$–F and the carbene H(F)B–C–H plausibly emerge as the most stable isomers, a variety of novel structural features emerge for the assembled energy minima of at least 16 species. All of these species are compared as well as transition states that connect them. Comparison is made with corresponding forms of the singlet species with this stoichiometry, shown earlier by us to have a rich diversity of structures as well as a large range of energies and relative stabilities.

1. Introduction

The isomeric compounds with the formula [B, C, F, H_2] are formally among the simplest species containing each of the elements together: boron, carbon, fluorine and hydrogen. They are the simplest such species for which the question of spin state naturally emerges [1]. The formally doubly bonded $H_2C{=}B{-}F$ is logically a closed-shell singlet, analogous to the isoelectronic diazomethane and ketene. The corresponding triplet, roughly drawn as the biradical $H_2C^{\bullet}$–$B^{\bullet}$–F, is expected to be a weakly bound, excited state corresponding to the excited states of diazomethane and ketene en route to triplet CH_2 as they photolytically dissociate [2]. The structurally related carbene H_2B–C–F with the boron and carbon transposed is plausibly a ground state triplet as we recognize this species to be a substituted derivative of the parent carbene, CH_2. Indeed this isomer was quite dominant in earlier literature discussions of [B, C, F, H_2] [3,4], even though our more exact calculations failed to confirm it to be a minimum on the singlet potential energy surface [1]. Any of our earlier hydrogen bridged or hydrogen bonded complexes containing CH_2, CHF or BH, might also be expected to have triplet counterparts as all of these fragments have energetically low lying states with unpaired electrons [5–7]. Summarizing our query, what are the structure and energetics of open-shell [B, C, F, H_2]?

To our knowledge, the only earlier computational study of triplet species with the formula [B, C, F, H_2] is that of Lanzisera and Andrews [3], in which they evaluated the triplet–singlet energy difference for H_2CBF. The calculations were performed to complement their matrix isolation study of reactions between laser-ablated boron atoms and CH_3X, X = F, Cl, Br. More computational work has been carried out on some of the boron-containing fragments relevant to the [B, C, F, H_2] species. Much of the recent work has focused on the thermochemical properties of these fragment species, in particular their atomization energies, enthalpies of formation, bond dissociation enthalpies BDHs, and excitation energies [8–16]. Most recently, Grant and Dixon [9] have reported these thermochemical data for $H_{(3-n)}BX_n$ compounds for which X is F, Cl, Br, I, NH_2, OH and SH (where $1 \leq n \leq 3$), using the composite ab initio molecular orbital theory approach Feller et al. are developing, which allows them to calculate thermochemical

* Corresponding author. Tel.: +1 573 882 1347; fax: +1 573 882 2754.
** Corresponding author. Tel.: +1 410 455 2549; fax: +1 410 455 2608.
E-mail addresses: deakynec@missouri.edu (C.A. Deakyne), jliebman@umbc.edu (J.F. Liebman).

0022-1139/$ – see front matter © 2009 Elsevier B.V. All rights reserved.
doi:10.1016/j.jfluchem.2009.07.006

properties to near chemical accuracy (±6.5 kJ/mol). (See for example Ref. [10] and references cited therein.) Earlier calculations on these and related cyclic and acyclic borane molecules and radicals were performed by Raabe et al. [11], Poon and Mayer [12], and Rablen and Hartwig [13]. Barreto et al. [14] have provided polynomial fits to the thermochemical data they computed for a series of chemical species, important in the growth of boron nitride thin films, containing B, H, N and F atoms. Bond dissociation enthalpies of a wider range of molecules, those involving all possible A–X single bonds between first- and second-row atoms, have been evaluated by Mó, et al. [15]. Ponomarev et al. [8] have examined the thermodynamic stabilities of bi- and triradicals derived from halogenated molecules of main group elements.

Most of the above articles include a discussion of trends in sequential bond dissociation enthalpies and/or trends in bond dissociation enthalpies along the periodic table. Comparison of B–X bond dissociation enthalpies, X = H, C, F, Cl, Br, I, in analogous compounds has shown that (1) BDHs decrease down the group from F to I [9,11], (2) B–H and B–C bond strengths are similar in magnitude but much smaller than B–F bond strengths [9,12–15], (3) the strengths of B–H and B–C bonds tend to be less dependent on the other boron substituents than do boron–halogen bonds [9,13,14], and (4) replacing a halogen substituent with hydrogen generally increases the BDHs of boron–halogen bonds [9,11,14]. However, because sequential adiabatic BDHs often have large fluctuations resulting from reorganization energy in the product fragments, the authors of some of these articles suggest that intrinsic bond strengths should be compared by evaluating diabatic BDHs [9,12,17] or the electron density at the bond critical point [15].

2. Computational details

All molecular geometries were fully optimized at the MP2/aug-cc-pVDZ level of calculation using the Gaussian 03 program package [18]. Tight convergence criteria were used for the optimizations. Harmonic vibrational frequencies were calculated to ensure stationary points were either minima or transition structures and to evaluate the thermal correction terms. Transition structures were searched for using the QST2 method [19,20] and intrinsic reaction coordinate, IRC, calculations [21–23] were performed on the transition structures located to confirm which minima each connected. Higher level single-point CCSD(T) energies were calculated with the basis sets aug-cc-pVXZ, X = D, T and Q, to estimate total energies at the complete basis set (CBS) limit. For the open-shell systems, the single-point energies were obtained using the fully unrestricted formalism (UHF, UCCSD(T)). The equation used to extrapolate to the CBS energy is that of Peterson et al. [24] (Eq. (1)) in which X = 2 (DZ), 3 (TZ), or 4 (QZ). The CCSD(T)//CBS total electronic energies, enthalpies and free energies can be found in Table S1 of the Supplementary material; Table S2 gives the unscaled MP2/aug-cc-pVDZ harmonic vibrational frequencies.

$$E(X) = E_{\mathrm{CBS}} + A\,e^{-(X-1)} + B\,e^{-(X-1)^2} \quad (1)$$

T_1 diagnostic values were computed at the CCSD(T)/aug-cc-pVDZ level to assess the possibility of non-trivial multireference character in the wave functions [25]. All of the T_1 diagnostics are 0.03 or below (see Table S3 of the Supporting material), indicating that these wave functions are dominated by a single configuration.

Following the protocol developed by Feller et al., the total atomization energy ΣD_0 of a compound is given by Eq. (2). (See for example Refs. [9,10,26].)

$$\Sigma D_0 = \Delta E_{\mathrm{elec}}(\mathrm{CBS}) - \Delta E_{\mathrm{ZPE}} + \Delta E_{\mathrm{CV}} + \Delta E_{\mathrm{DKH\text{-}SR}} + \Delta E_{\mathrm{SO}} \quad (2)$$

The last three terms in Eq. (2) contribute small corrections to the total atomization energy. Component ΔE_{CV} accounts for core–valence correlation energy effects and was obtained as the difference between the CCSD(T)(CV)//cc-pwCVTZ and CCSD(T)(FC)//cc-pwCVTZ energies [27]. Douglas–Kroll–Hess [28,29] scalar relativistic corrections $\Delta E_{\mathrm{DKH\text{-}SR}}$ were evaluated with the DKH implementation of Gaussian 03 at the CCSD(T)(FC)//cc-pVTZ-DK level of theory [30]. The term ΔE_{SO} gives the contribution of the atomic spin–orbit coupling to the atomization energy. The spin–orbit corrections, from the tabulated values of Moore [31], are −0.93 kJ/mol for B, −0.36 kJ/mol for C and −1.59 kJ/mol for F. To calculate ΔE_{ZPE} in Eq. (2), the C–H stretches were scaled by the factor of 0.9701 suggested by Matus et al. [26] in their theoretical study of the thermochemical properties of CHFO and CFO.

Molecular enthalpies of formation at 0 K were computed from the total atomization energies and the experimental enthalpies of formation at 0 K [32] for the atoms H (216.0 kJ/mol), C (711.2 kJ/mol) and F (77.27 kJ/mol). The value of $\Delta_f H$ = 565.3 kJ/mol for B was taken from Ref. [33]. Enthalpies of formation at 298 K were assessed following the procedure established by Curtiss et al. [34].

NBO [35,36] and AIM [37] analyses were carried out to obtain information on bonding. The AIM analysis was used to determine the presence of bond critical points and the magnitude of the bond critical point density. The bond critical point density is the electron density $\rho(\mathbf{r})$ at the unique point at which the bond path between two atoms intersects the interatomic surface [37]. This electron density ρ_b is often used as a measure of the strength of the bond between the atoms [15,38,39]. The NBO analysis of the Hartree-Fock orbitals was used to examine the influence of hyperconjugative effects on the stabilities of the hydrogen-bonded and van der Waals complexes identified in this work. Orbital interaction energies $\Delta E^{(2)}$ (donor → acceptor) were estimated with the second-order NBO perturbation approach [36]. For many of these complexes, the largest interaction energy is associated with a lone pair or unpaired electron on atom Y delocalizing into an unfilled H–X natural bond orbital, a $n(\mathrm{Y}) \rightarrow \sigma^*(\mathrm{H\text{–}X})$ hyperconjugation. For the remaining complexes, the dominant contribution to $\Delta E^{(2)}$ is from a $\sigma(\mathrm{Y\text{–}Z}) \rightarrow \sigma^*(\mathrm{H\text{–}X})$ hyperconjugation, involving delocalization of electron density from a filled Y–Z orbital into an unfilled H–X orbital.

3. Results and analysis of results

3.1. Minima and transition structures identified

3.1.1. Minima

Sixteen minima have been located for open-shell [B, C, F, H_2]. As in all computational studies of this nature there is always the possibility that minima have not been identified and that some of those found will collapse. In fact, we have located two new minima on the singlet potential energy surface PES of [B, C, F, H_2] as a result of the triplet investigation. We also have evidence that one triplet may collapse to a related minimum when re-optimized at a higher level of theory (see below).

The triplet isomeric structures depicted in Fig. 1 are arranged in order of decreasing stability. The two new singlet isomeric structures have also been included in the figure. All bonds shown in the figure were confirmed by AIM analysis [37]. Geometrical parameters for each of the 18 minima and related fragment species are collected in Table 1.

A wide range of acyclic connectivities was found for the open-shell [B, C, F, H_2] stoichiometry. We have chosen semi-systematic designations for our minima, realizing that proper names are often cumbersome and not designed for most of our species. As with the singlets [1], no cyclic triplet compounds are at minima. Unlike the

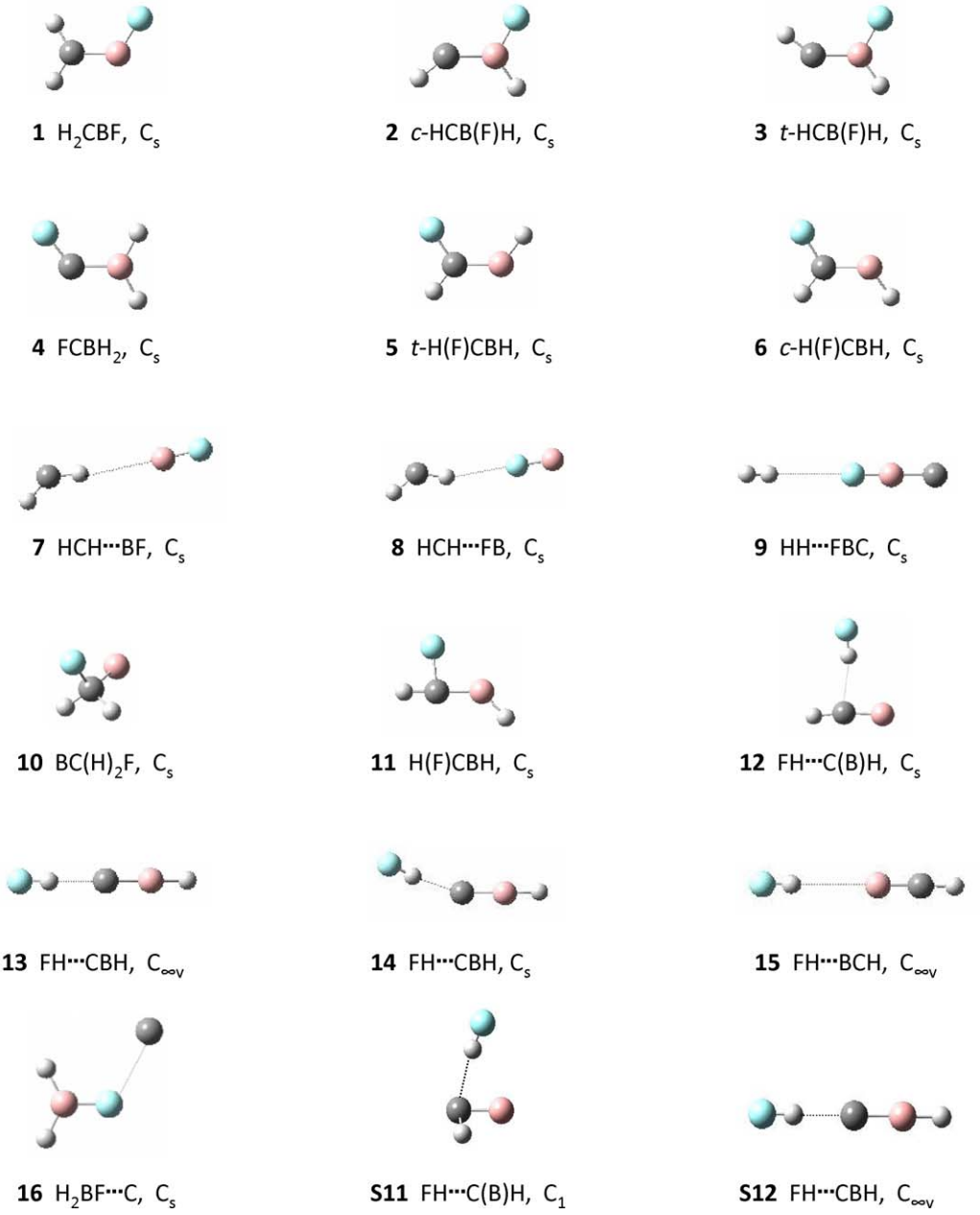

Fig. 1. Structures of the 16 isomers located on the triplet potential energy surface and two additional singlets. C: grey, H: white, B: pink, F: cyan. (For grayscale, the degrees of coloration are C > B > F > H.) (For interpretation of the references to color in this figure legend, the reader is referred to the web version of the article.)

singlets, no fluorine-bridged triplet compounds are at minima. Many of the isomers that were located display conventional covalent bonding; most of the remaining, more loosely bound isomers display conventional or unconventional hydrogen bonding. Three of the covalently bound structures are the partially bond-ruptured excited ketene- and diazomethane-like **1** $H_2C^{\bullet}$–$B^{\bullet}$–F, analogous to **S1** H_2C=B–F on the singlet PES, and the related partially bond-ruptured **5** *t*-H(F)$C^{\bullet}$–$B^{\bullet}$–H and **6** *c*-H(F)$C^{\bullet}$–$B^{\bullet}$–H, analogous to **S2** H(F)C=B–H. (Note: in this article species denoted without a letter prefix are triplet minima. Singlet minima [1] will be denoted with the prefix "S" to distinguish them from the triplet species.) Isomer **11** H(F)CBH is an oddly shaped molecule with the same connectivity as **5** and **6** but a linear HCB angle (Table 1 and Fig. 1). The odd shape led us to re-optimize the geometry of **11** at the CCSD/aug-cc-pvdz level of theory, and at this calculational level **11** collapses to **6**. That the C–B–X angle, X = F, H, is $<180^{\circ}$ in **1**, **5** and **6** is indicative of the unpaired electron occupying an sp^2-orbital rather than a p-orbital on boron and gives rise to the possibility of three-coordinated boron species. Exchange of the boron and carbon atoms in **5**, **6**, and **1** yields the carbenes **2** *c*-HCB(F)H, **3** *t*-HCB(F)H, and **4** $FCBH_2$, respectively. The latter three structures have no singlet counterparts. The only four-coordinated carbon atom is found in **10** $BC(H)_2F$, which is related to **S3** $BC(H)_2F$. Overall, in contrast to the singlets [1], with the exception of a four-coordinate boron atom, all possible arrangements of the remaining atoms on boron and carbon are observed for open-shell [B, C, F, H_2].

Turning now to the hydrogen-bonded species, **7** and **8** consist of a CH_2 group loosely bound through an unconventional C–H···Y hydrogen bond. Boron is the electron-donating atom Y in **7** H_2C···BF and fluorine is the electron-donating atom in **8** H_2C···FB. The series of molecules **12**–**15** contain conventional hydrogen bonds with HF as the proton donor. In isomers **12** FH···C(B)H and **15** FH···BCH the fragment HCB is the proton acceptor, through the C for **12** and B for **15**. Complex **12** FH···C(B)H is unique among the

Table 1
Geometrical parameters[a].

Isomer	Bond lengths	Bond angles	Dihedral angles
1 H_2CBF, C_s	CB: 1.542 BF: 1.356 CH: 1.096 CH_1: 1.091	HCB: 121.8 H_1CB: 122.1 CBF: 121.9	HCBF: 0.0
2 *c*-HCB(F)H, C_s	CB: 1.534 BF: 1.362 CH: 1.090 BH: 1.204	HCB: 141.0 CBH: 123.3 CBF: 119.5	HCBF: 180.0
3 *t*-HCB(F)H, C_s	CB: 1.535 BF: 1.368 CH: 1.090 BH: 1.200	HCB: 143.1 CBH: 123.5 CBF: 119.2	HCBF: 0.0
4 $FCBH_2$, C_s	CB: 1.526 CF: 1.326 BH: 1.202 BH_1: 1.196	CBH: 118.2 CBH_1: 118.0 FCB: 128.2	FCBH: 0.0
5 *t*-H(F)CBH, C_s	CB: 1.511 CF: 1.361 CH: 1.094 BH: 1.196	FCB: 121.9 HCB: 128.2 CBH: 128.6	FCBH: 0.0
6 *c*-H(F)CBH, C_s	CB: 1.511 CF: 1.352 CH: 1.097 BH: 1.197	FCB: 121.2 HCB: 128.9 CBH: 125.3	FCBH: 180.0
7 $H_1CH\cdots BF$, C_s	BF: 1.302 CH: 1.089 CH_1: 1.089 H···B: 2.900	H_1CH: 133.2 CH···B: 174.8 H···BF: 175.8	CH···BF: 0.0 $H_1CH\cdots B$: 180.0
8 $H_1CH\cdots FB$, C_s	BF: 1.305 CH: 1.088 CH_1: 1.088 H···F: 2.602	H_1CH: 132.7 CH···F: 163.7 H···FB: 179.7	CH···FB: 180.0 $H_1CH\cdots F$: 180.0
9 HH···FBC, C_s	CB: 1.485 BF: 1.305 HH: 0.755 F···H: 2.833	CBF: 180.0 BF···H: 179.9 F···HH: 179.8	BF···HH: −2.2 CBF···H: 3.1
10 $BC(H)_2F$, C_s	CB: 1.550 CF: 1.431 CH: 1.105	FCB: 115.5 HCF: 106.9 HCB: 109.8	HCBF: ±121.0 HCBH: 118.1
11 H(F)CBH, C_s	CB: 1.512 CF: 1.503 CH: 1.093 BH: 1.197	FCB: 95.9 HCB: 180.0 CBH: 132.4	HCBH: −89.9 FCBH: 180.0 FH···CB: 180.0
12 $FH\cdots C(B)H_1$, C_s	CB: 1.374 CH_1: 1.082 H···C: 2.062 HF: 0.941	H_1CB: 171.9 H···CB: 88.1 FH···C: 170.4	
13 FH···CBH, $C_{\infty v}$	CB: 1.457 BH: 1.183 H···C: 1.832 HF: 0.952		
14 FH···CBH, C_s	CB: 1.458 BH: 1.183 H···C: 1.848 HF: 0.951	CBH: 176.3 H···CB: 158.8 FH···C: 171.4	H···CBH: 0.0 FH···CB: 0.0
15 FH···BCH, $C_{\infty v}$	CB: 1.359 CH: 1.080 H···B: 2.758 HF: 0.926		
16 $H_2BF\cdots C$, C_s	BF: 1.362 BH: 1.200 BH_1: 1.200 F···C: 2.543	FBH: 117.2 FBH_1: 116.8 BF···C: 118.1	C···FBH: 0.0
S11 $FH\cdots C(B)H_1$, C_1	C···B: 1.412 CH_1: 1.176 C···H: 2.099	B···CH_1: 77.3 B···C···H: 74.5 FH···C: 172.1	FH···C···B: 14.7 FH···CH_1: 87.7
	HF: 0.939	H···CH_1: 102.0	
S12 FH···CBH, $C_{\infty v}$	CB: 1.478 BH: 1.182 H···C: 1.853 HF: 0.949		
TS 1–2, C_1	CB: 1.491 BF: 1.361 CH: 1.091 C···H: 1.488 B···H: 1.315	CBF: 127.1 HCB: 140.0 C···H···B: 63.9	FBCH: 169.4 FBC···H: 123.1
TS 1–3, C_1	CB: 1.478 BF: 1.361 CH: 1.099 C···H: 1.525 B···H: 1.318	CBF: 132.7 HCB: 144.1 C···H···B: 62.1	FBCH: −16.9 FBC···H: −123.4
TS 2–3, C_1	CB: 1.523 BF: 1.366 CH: 1.082 BH: 1.201	HCB: 180.0 CBF: 119.7 CBH: 123.5	FBCH: −89.5
TS 4–5, C_1	CB: 1.489 CF: 1.331 BH: 1.197 C···H: 1.512 B···H: 1.314	CBH: 127.4 FCB: 130.5 C···H···B: 63.1	FCBH: −7.1 FCB···H: 105.8
TS 4–6, C_1	CB: 1.504 CF: 1.330 BH: 1.191 C···H: 1.460 B···H: 1.319	CBH: 123.8 FCB: 125.2 C···H···B: 65.3	FCBH: 178.1 FCB···H: 72.8
TS 5–6, C_s	CB: 1.479 CF: 1.372 CH: 1.095 BH: 1.178	CBH: 177.4 FCB: 122.1 HCB: 129.9	FCBH: 180.0
TS 1–5, C_1	C···B: 1.766 CH: 1.115 BF: 1.506 C···F: 1.719 C···H: 1.430 B···H: 1.285	HC···H: 124.4 H···BF: 96.1 C···H···B: 80.9	HC···BF: 96.8 FB···C···H: −122.3
TS 3–5, C_s	CB: 1.404 CH: 1.080 BH: 1.178 C···F: 1.854 B···F: 2.150	HCB: 171.6 CBH: 179.7 F···CB: 81.3 C···F···B: 40.2	F···CBH: 180.0 HCBH: 0.0
TS 1–10, C_s	CB: 1.445 CH: 1.093 C···F: 1.849 B···F: 2.151	BCH: 120.7 HCH: 117.6 F···CB: 80.5 HC···F: 99.8	HCB···F: ±95.9 HCH···F: 106.6 BCH···F: 84.7 BCHH: −168.6
TS 6–10, C_1	CB: 1.462 CF: 1.380 CH: 1.099 C···H: 1.508 B···H: 1.312	FCB: 124.0 FCH: 107.7 BCH: 127.9 FC···H: 127.3 BC···H: 52.4	HCB···H: 58.4 FCH···H: 130.7 BCF···H: 65.7 BCFH: 173.5
^3BF ^3BH ^2CH ^2CF	BF: 1.353 BH: 1.198 CH: 1.130 CF: 1.300		
$^2BH_2$ $^3CH_2$	BH: 1.173 CH: 1.088	HBH: 104.3 HCH: 132.6	
^3HCF	CF: 1.339 CH: 1.095	HCF: 121.0	
^3CBH	CB: 1.468 BH: 1.186	CBH: 180.0	
^3BCH	CB: 1.363 CH: 1.081	BCH: 180.0	
^3CBF	CB: 1.485 BF: 1.305	CBF: 180.0	

Table 1 (*Continued*)

Isomer	Bond lengths	Bond angles	Dihedral angles
^{2}HBF	BH: 1.209 BF: 1.343	HBF: 120.5	
$^{3}H_2BF$, C_s	BH: 1.303 BF: 1.367	FBH: 115.6 HBH: 58.2	FBHH: ±105.5

[a] Bond lengths in Å, bond angles and dihedral angles in degrees.

hydrogen-bonded complexes, with its connection between HF and the medial fragment atom and consequent T-shaped structure. When the triatomic HBC is the proton acceptor (**13** and **14**), only FH···C hydrogen bonds are observed. Isomer **14** FH···CBH, C_s has the same connectivity as **13** FH···CBH, $C_{\infty v}$, but with a bent H···CB bond angle (Table 1 and Fig. 1).

The new isomers on the singlet PES, **S11** FH···C(B)H and **S12** FH···CBH, have FH···C linkages with HCB and HBC, respectively, and correlate with **12** and **13**, respectively. The only other singlet–triplet hydrogen-bonded pairs are **S4**, **7** and **S5**, **8** [1]. It must be noted that AIM analysis [37] finds no bond path linked to boron in **S11**, despite a shorter C–B distance in this molecule than in **S12** and most of the triplet molecules (Table 1). When the geometry of **S11** was re-optimized at the CCSD/aug-cc-pVDZ level of theory, a C_1 structure more similar to that of its triplet counterpart **12** was obtained (e.g., C–H_1 = 1.089 Å, <BCH_1 = 128.6°). At this calculational level, a bond path does exist between the B and C.

The last two triplet structures identified are van der Waals complexes. Structure **9** HH···FBC has a hydrogen molecule interacting with the fluorine end of the triatomic FBC and is analogous to the singlet **S9** HH···FBC [1]. As a boron-centered planar complex, **16** H_2BF···C is a surprising minimum with the fluorine loosely bound to the carbon 2.554 Å away (Table 1 and Fig. 1).

3.1.2. Transition structures

In our search for transition structures connecting the minima, we focused on those isomers for which rearrangement rather than fragmentation may be more likely. The most relevant isomerization pathways are illustrated in Fig. 2; each pathway is endothermic as written. Bond lengths, bond angles and dihedral angles for the transition structures can be found in Table 1. The label associated with each transition structure designates the minima it connects. Conversion between the cis and trans isomers of HCB(F)H or H(F)CBH proceeds through **TS 2–3** or **TS 5–6** (Fig. 2A and B), which have the expected linear HCB angle (**TS 2–3**) and nearly linear HBC angle (**TS 5–6**, Table 1). Other transition structures that concur with chemical intuition include **TS 1–3** and **TS 4–5** (Fig. 2A and B). Both of these rearrangements involve the transfer of a hydrogen atom between the carbon and boron. In each case as the hydrogen shifts along the C–B bond, it remains on the same side of the bond on which it started. It does, however, move out of the molecular plane. The **1–2** and **4–6** rearrangements require the hydrogens, which start out on the same atom, to end up in the cis configuration. The transition structures show the out-of-plane movement of the hydrogen as it crosses the C–B bond. The geometries of all four of these transition structures are similar in that the B···H distance is ~1.3 Å, the C···H distance is ~1.5 Å and the B···H···C angle is ~65°. In addition, the angle the "immobile" hydrogen makes with B and C has opened up to within ~1° of its value in the product (Table 1). The straightforward B → C shuttling of the fluorine or hydrogen atom observed in **TS 1–10** and **TS 6–10** (Fig. 2E and F) leads to rehybridization of the carbon atomic orbitals. The atom that is shifting has moved out of the molecular plane, but the pyramidalization of the H_2CB geometry has not yet occurred. Similar structural features were found in the transition

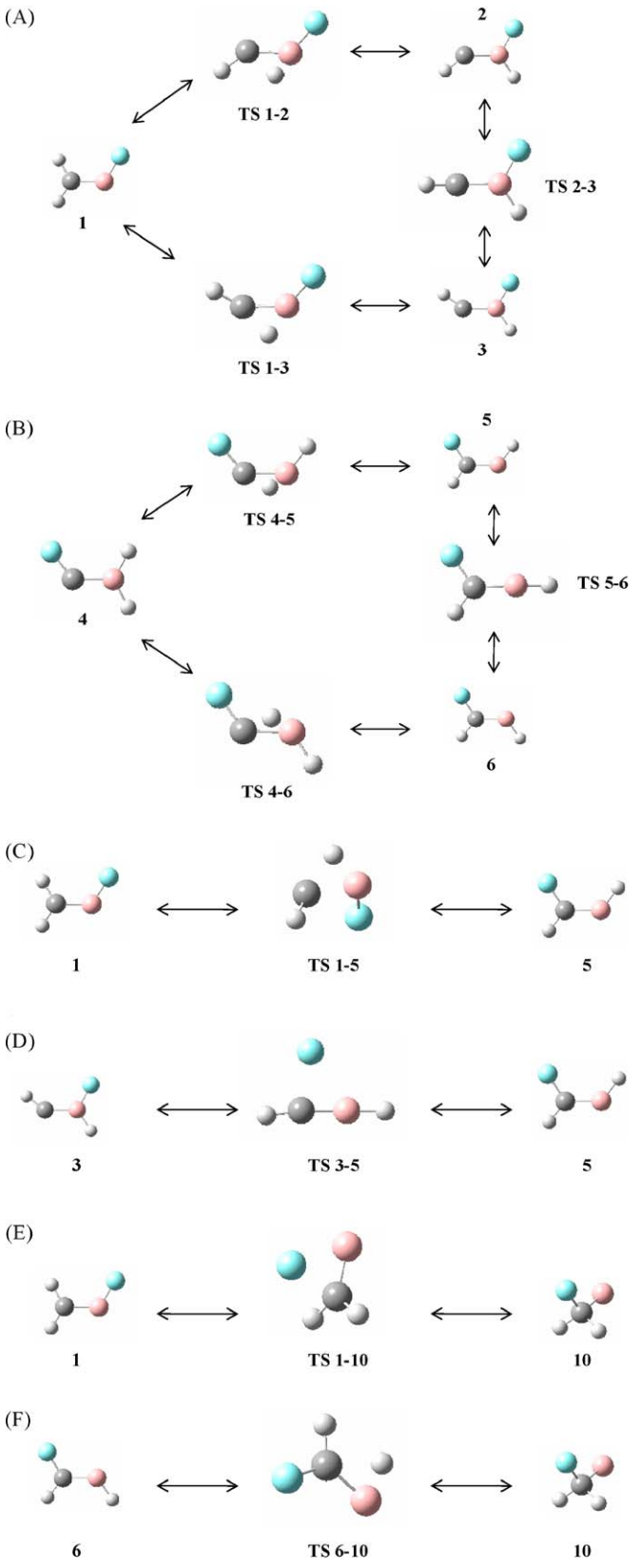

Fig. 2. Transition states and the minima they connect. C: grey, H: white, B: pink, F: cyan. (For grayscale, the degrees of coloration are C > B > F > H.) (For interpretation of the references to color in this figure legend, the reader is referred to the web version of the article.)

structures connecting the analogous singlet minima, **S1–S3** and **S2–S3** [1].

One of the more unexpected characteristics of **TS 1–5** is that the hydrogen is inserted between the C and B stretching the C–B bond (Fig. 2C). Also, in order to effect a transition in which the exchanging H and F atoms end up on the same side of the C–B bond, the HC and BF fragments twist perpendicularly (<HC···BF = 96.8°, Table 1). Overall, the **1–5** isomerization occurs in a stepwise manner; the B–H bond is within 7% of its equilibrium distance in **5** and the B–F bond is stretched by only 11%. In **TS 3–5** the fluorine is displaced by 37% from the C–F bond distance in **5** and the hydrogens, initially trans, have flattened out to within 10° of linearity to facilitate their rotation about the B–C bond when the fluorine transfer is complete.

Other than the cis–trans interconversions, each of the reactions depicted in Fig. 2 possesses a transition structure shifted toward a "later", more product-like position, on the reaction coordinate. Nevertheless, not all of these reactions obey the Leffler–Hammond postulate [40,41] because some of the most product-like transition structures are associated with the reactions that are essentially thermoneutral (see below).

3.2. Energetics

3.2.1. Minima

3.2.1.1. Triplet–triplet and singlet–triplet energy gaps. The energies, enthalpies and free energies of the triplet minima relative to the corresponding values for **1** H_2CBF are given in Table 2. The data for the two new singlet minima relative to that for **S1** H_2CBF are also included in the table. The relative enthalpies of the set of triplet [B, C, F, H_2] isomers are compared with those of the set of singlet [B, C, F, H_2] isomers in Fig. 3 (this work and Ref. [1]). The singlet isomers have not been renumbered with respect to relative energy, so the grouping in Fig. 3 that lies at ca. 600 kJ/mol represents **S11** FH···C(B)H, **S7** H(C)BFH and **S12** FH···CBH, respectively.

The entropy term (298 K) makes only a minor contribution to the relative stabilities of many of these species but when it does have a non-negligible effect, it stabilizes the species with respect to **1** H_2CBF (Table 2). Because the relative enthalpies of some of these minima are clustered so closely together, the trends in ΔH and ΔG are similar but not identical. Isomers **9** HH···FBC and **10** $BC(H)_2F$ account for the only deviation in relative enthalpies between the MP2 and CCSD(T) methods. At the MP2/aug-cc-pVDZ level of calculation, the hydrogen-bonded isomer **9** is about 13 kJ/mol less stable than **10**, the only isomer with a four-coordinate carbon. However, this difference is reversed by ca. 25 kJ/mol at the CCSD(T) level.

Table 2
Relative thermochemical data for minima identified[a,b].

Isomer	ΔE	$\Delta(E+ZPE)$	$\Delta_{298}H$	$\Delta_{298}G$
1 H_2CBF	0.0	0.0	0.0	0.0
2 *c*-HCB(F)H	10.7	5.9	5.8	5.9
3 *t*-HCB(F)H	13.6	9.0	8.8	8.7
4 $FCBH_2$	195.9	189.3	189.1	189.5
5 *t*-H(F)CBH	196.8	194.5	194.0	194.6
6 *c*-H(F)CBH	197.5	194.9	194.4	195.3
7 HCH···BF	268.6	250.3	257.7	236.5
8 HCH···FB	271.3	251.6	260.1	234.5
9 HH···FBC	298.8	271.1	278.9	271.3
10 $BC(H)_2F$	301.0	303.1	302.4	303.3
11 H(F)CBH	332.3	323.4	324.0	322.9
12 FH···C(B)H	342.4	334.6	337.9	328.7
13 FH···CBH, $C_{\infty v}$	354.4	344.1	347.2	342.8
14 FH···CBH, C_s	356.4	345.4	347.8	341.4
15 FH···BCH	361.7	351.6	359.1	339.1
16 H_2BF···C	385.0	370.7	374.7	361.9
S11 FH ···C(B)H[c]	599.0	588.2	591.1	580.2
S12 FH···CBH	613.5	603.1	606.3	599.0

[a] CCSD(T)/CBS data in kJ/mol.
[b] Energies for **1** in hartrees are $E = -163.7543384$, $E+ZPE = -163.7256481$, $H_{298} = -163.7210084$, and $G_{298} = -163.7511744$.
[c] **S11** and **S12** energies are relative to the ground-state singlet. Energies [1] for **S1** in hartrees are $E = -163.8217944$, $E+ZPE = -163.7932734$, $H_{298} = -163.7884414$, and $G_{298} = -163.8167594$.

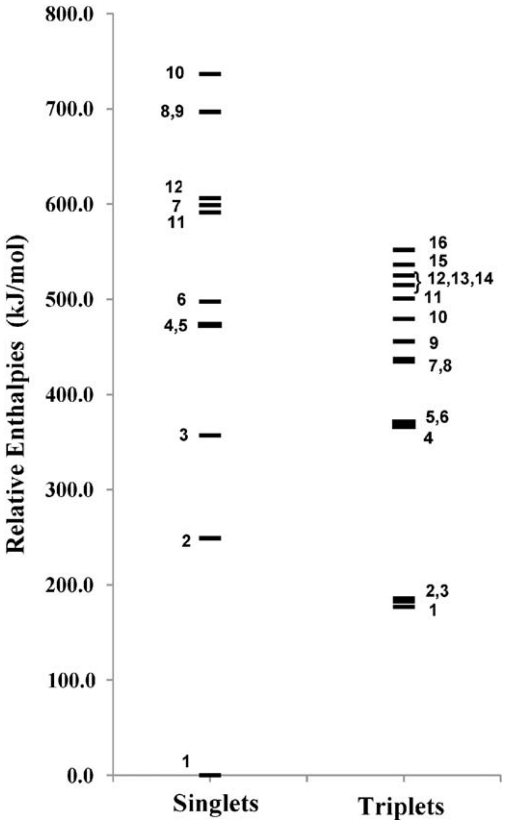

Fig. 3. Comparison of the relative enthalpies of isomers on the singlet [1] and triplet potential energy surfaces. Dotted lines connect analogous isomers of different multiplicities.

Among the conventionally bound triplets, the CBF connectivity is more favorable than the FCB connectivity. As it was for the analogous singlets [1], this preference can be rationalized primarily on the basis of the greater strength of the B–F bond compared to that of the B–H bond [9,12–15,42]. The stabilities of **5** *t*-H(F)CBH (**6** *c*-H(F)CBH) relative to **1** H_2CBF and of **S2** H(F)CBH relative to **S1** H_2CBF are not greatly different in magnitude (195 kJ/mol vs. 250 kJ/mol, this work and Ref. [1]). A similar difference in stability is found between **4** $FCBH_2$ and **2** *c*-HCB(F)H (**3** *t*-HCB(F)H), ca. 180 kJ/mol (Table 2). Given the CBF or FCB connectivity, however, rearrangement of the hydrogens on the C and B atoms has little effect on stability; for each set of related isomers the enthalpies and free energies are all within 10 kJ/mol of each other. This result is consistent with the similar magnitudes of the CH (340–345 kJ/mol) and BH (341 kJ/mol) bond dissociation enthalpies derived from the relevant gas-phase enthalpies of formation in the NIST Chemistry WebBook [42]. Although evaluated at a lower level of theory, Schleyer and coworkers [43,44] obtained essentially equal energies for triplet H_2CBH and $HCBH_2$, suggesting that substituting F for H also has little effect on the relative stabilities of these species.

The most striking difference structurally in the two sets of cis and trans isomers is the magnitude of the HCB angle. This angle in **2** and **3** (and $HCBH_2$ [43]) is at least 12–15° closer to linear than is any angle in **5** and **6** (and H_2CBH [44]) (Table 1), which is one

manifestation of the greater concentration of p-character in the in-plane C orbital directed toward the unpaired electron than in the corresponding B orbital. The difference in hybridization around the central C and B atoms is consistent with Bent's rule [45], since carbon and hydrogen are more electronegative elements than is boron. The greater repulsion between the fluorine atom and unpaired electron in the oddly shaped isomer **11** H(F)CBH than in isomer **6** makes it about 130 kJ/mol less stable than **6**. The increased repulsion in **11** arises from its more acute <FCB, less acute <HBC, longer C–F bond (Table 1), and associated greater p-character in the C orbital directed toward the fluorine and B orbital directed toward the unpaired electron.

Triplet **10** $BC(H)_2F$ is closer in energy to triplet **1** H_2CBF than **S3** $BC(H)_2F$ is to **S1** H_2CBF [1], but **10** is less favorable than its singlet counterpart (Table 2 and Fig. 2). Replacing the fluorine atom with hydrogen decreases the observed energy gaps, for both the triplet and singlet species. The singlet–singlet and triplet–triplet separations are both less than 100 kJ/mol for BCH_3 vs. H_2CBH [44].

Interestingly, the cluster of complexes with unconventional hydrogen bonds, **7**–**9**, has lower total energies than the cluster of complexes with conventional hydrogen bonds, **12**–**15** (Table 2). In contrast, the energies of the conventionally hydrogen-bonded singlet complexes, **S11** FH···C(B)H and **S12** FH···CBH, lie between those of the two sets of unconventionally hydrogen-bonded singlet complexes [1] **S4** HCH···BF, **S5** HCH···FB and **S8** H_2···C(F)B, **S9** H_2···FCB (Fig. 3). Within each group of triplet complexes the stabilities differ by no more than 20 kJ/mol, whereas the separation between the groups is 60 kJ/mol. At the CCSD(T)/CBS level of calculation, the enthalpy difference $\Delta H[HBC(^3\Sigma^-) - HCB(^3\Pi)]$ = 27.1 kJ/mol, which is identical to the G3(MP2) value computed by Zeng et al. [16]. That **12** FH···C(B)H is only 10 kJ/mol more stable than **13** FH···CBH can be partially attributed to the 8° bending of the linear HCB fragment on complexation (Table 1). The van der Waals complex **16** H_2BF···C lies only 15 kJ/mol above the second cluster of hydrogen-bonded isomers (Fig. 2).

The enthalpies and free energies of the triplet minima are much more compressed than those of the singlet minima (Table 2, Fig. 2 and Ref. [1]). Although the three lowest lying [B, C, F, H_2] singlets are considerably more stable than the corresponding triplets, which was also observed for the [B, C, H_3] species [43,44], the trend is reversed for the more "physically" bound triplets and their corresponding singlets. This reversal produces a shift in the stability order for the two sets of isomers. Overall, the most stable [B, C, F, H_2] species is **S1** H_2CBF. Its enthalpy is 177 kJ/mol below that of triplet **1** and the enthalpies of triplets **1**–**3**, H_2CBF, *c*-HCB(F)H and *t*-HCB(F)H, are about 75 kJ/mol below that of **S2** H(F)CBH. At the MP2/D95* level of theory, Lanzisera and Andrews [3] found a similar difference of 163 kJ/mol in the energies of singlet and triplet H_2CBF.

Singlet–triplet splittings for the fragments relevant to the binding affinities discussed below are given in Table 3. Experimental and computed S–T splittings have been reported previously for several of these species, and the CCSD(T)/CBS values are included here for comparison and to provide the thermodynamic data required to compute diabatic bond dissociation enthalpies for the [B, C, F, H_2] isomers. A positive value for the S–T splitting signifies that the triplet lies higher in energy than the singlet.

Table 3
Singlet–triplet splittings[a,b].

Species	Δ(*E*+ZPE)	Species	Δ(*E*+ZPE)
BH	129.5	HBC	−77.7
BF	348.7[c]	HCB	−70.0
CH_2	−37.0	CBF	−85.2
HCF	62.8	H_2BF	410.4

[a] CCSD(T)/CBS values in kJ/mol.
[b] Negative values indicate that the triplet species is more stable.
[c] Ref. [9].

For CH_2 and HCF the CCSD(T)/CBS results are in excellent agreement with the results from both experiment (to within 1 kJ/mol, Refs. [5,6]) and the W1′ procedure (to within 1.5 kJ/mol, Ref. [46]). The discrepancy between the CCSD(T)/CBS and experimental (124.3 kJ/mol, Ref. [7]) singlet–triplet gaps for BH is somewhat larger at 5.2 kJ/mol, but the discrepancy is smaller between our value and the FCI/aug-cc-pVDZ value of 126.7 kJ/mol [47]. The tabulated singlet–triplet splitting for BF was reported earlier by Grant and Dixon [9].

3.2.1.2. Binding affinities. Photolytic decomposition of the excited states of ketene and diazomethane has been used as a source of $^3CH_2$ [2]. In triplet H_2CCO, the C–C adiabatic bond dissociation energy forming $^3CH_2$ and ^1CO is calculated to be 88.3 kJ/mol at the QCISD(T)/cc-pVQZ//B3LYP/cc-pVQZ level of theory [48], consistent with the expected weak binding in this system. On the other hand, the adiabatic B–C BDHs and bond critical point electron densities ρ_b in isomers **1**–**6** and **10** (and **11**) demonstrate that the binding in these systems is significantly tighter (Table 4), as has been observed for other corresponding first adiabatic C–C and B–C BDHs [13,15]. The strength of the B–C bonds in **1**–**6** and **10** is not unusual; the adiabatic BDHs in these molecules are comparable in magnitude to those in a number of organoborane closed- and open-shell species examined previously [1,12,13,15,49]. For example, our calculated adiabatic B–C BDHs are 443.4 and 489.6 kJ/mol in the neutral species **S1** H_2CBF and **S2** H(F)CBH, respectively [1] and are 373 and 447 kJ/mol (with a smaller basis set) in the triplet ionic species $HBCN^-$ and $HBCF^+$, respectively [49]. Other reported examples of adiabatic B–C BDHs in closed-shell organoboranes include the G3 value [12,15] of 434.9 kJ/mol in H_2BCH_3 and the G2 values [13] of 465.3 kJ/mol in F_2BCH_3 and 384.5 kJ/mol in BCH_3. The corresponding G2 adiabatic B–C BDH in $^3BCH_3$ is 202.1 kJ/mol [13], implying that fluorination has stabilized the triplet with respect to the singlet since the decrease in bond strength on excitation is 122 kJ/mol for **S3** $BC(H)_2F$ and **10** [1]. Further comparison can be made with our calculated BDHs in ^3HCB (501.7) and ^3HBC (467.6 kJ/mol), which are at the high end of the range of values in Table 4. The dissociation energy D_e in ^3HBC is 479.4 kJ/mol, in excellent agreement with the MRCI + Q/[(cc-pVQZ)$_H$/(cc-pV5Z-h)$_{B,C}$] theoretical value of 477 kJ/mol reported by Tzeli and Mavridis [50]. Overall, as we have suggested previously [1,49], with such tight boron–carbon bonds these species are "chemically" bound and should be considered new and different species.

Although the B–C bond in **1** H_2CBF is apparently 2–3 times stronger than the C–C bond in ketene, it is dramatically weaker than the B–C bonds in the related isomers **2**–**6** and even **11** (Table 4). As has been pointed out for similar systems, the lower adiabatic B–C BDH in **1** results from the unusual stability of the closed-shell singlet BF product [9,12,13]. Use of a diabatic process [9,17], which accounts for the reorganization enthalpy of the product fragments, will perhaps yield a more appropriate comparison of the B–C bond strengths. The diabatic BDH gives a better estimate of the intrinsic or instantaneous strength of a bond, as does the bond critical point electron density ρ_b [15]. Focusing on **1** H_2CBF and **5** *t*-H(F)CBH, for which there are corresponding singlets, as defined by Dixon and coworkers [9,17] the diabatic process involves formation of ^3BX where one unpaired electron comes from the radical reactant and one from the bond breakage. From the singlet–triplet splittings in Table 3, the diabatic B–C BDHs in **1** and **5** are 615 and 560 kJ/mol, respectively. The analogous dissociation channels in **S1** H_2CBF and **S2** H(F)CBH are 792 and 682 kJ/mol, respectively (this work and Ref. [1]). The differences in

Table 4
Reaction thermochemistry: adiabatic bond dissociations.[a].

Reaction	$\Delta_{rxn}E$	$\Delta_{rxn}(E+ZPE)$	$\Delta_{rxn}H$	$\Delta_{rxn}G$	ρ_b[b]
1 $CH_2BF \rightarrow {}^3CH_2 + {}^1BF$	272.9	251.1	257.6	218.6	0.182 [0.225]
2 *c*-HCB(F)H $\rightarrow {}^2HC + {}^2FBH$	493.2	469.2	475.8	434.0	0.179
3 *t*-HCB(F)H $\rightarrow {}^2HC + {}^2FBH$	490.3	466.1	472.8	431.1	0.179
4 $FCBH_2 \rightarrow {}^2CF + {}^2BH_2$	369.4	346.6	353.3	310.6	0.170 [0.222]
5 *t*-H(F)CBH $\rightarrow {}^3FCH + {}^1BH$	448.7	423.3	430.3	388.6	0.191
6 *c*-H(F)CBH $\rightarrow {}^3FCH + {}^1BH$	448.1	422.9	429.9	388.0	0.184
7 HCH···BF $\rightarrow {}^3CH_2 + {}^1BH$	4.0	0.8	−0.1	−17.9	0.00572
8 HCH···FB $\rightarrow {}^3CH_2 + {}^1BH$	1.3	−0.4	−2.5	−15.9	0.00448
9 HH···FBC $\rightarrow {}^3CBF + {}^1H_2$	0.5	−1.9	−2.2	−25.6	0.00264
10 $BC(H)_2F \rightarrow {}^2CH_2F + {}^2B$	215.0	203.6	208.7	173.8	0.181 [0.183]
11 H(F)CBH $\rightarrow {}^3FCH + {}^1BH$	313.2	294.4	300.3	260.3	0.175
12 FH···C(B)H $\rightarrow {}^3HCB + {}^1HF$	21.4	16.5	19.3	−7.5	0.0250
13 FH···CBH, $C_{\infty}V \rightarrow {}^3HBC + {}^1HF$	43.2	33.9	37.0	4.9	0.0400
14 FH···CBH, $C_s \rightarrow {}^3HBC + {}^1HF$	41.2	32.7	36.4	6.4	0.0382
15 FH···BCH $\rightarrow {}^3HCB + {}^1HF$	2.2	−0.5	−2.0	−17.9	0.00543
16 $H_2BF\cdots C \rightarrow {}^1H_2BF + {}^3C$	7.2	5.6	5.8	−14.7	0.0142
S11 FH···C(B)H $\rightarrow {}^1HCB + {}^1HF$	20.9	10.5	13.9	−18.4	[0.0260] (0.0192)[c]
S12 FH···CBH $\rightarrow {}^1HBC + {}^1HF$	38.8	29.8	32.7	1.3	[0.0359]

[a] CCSD(T)/CBS//MP2/aug-cc-pVDZ data in kJ/mol.
[b] Bond critical point electron density, in a.u., for the bond broken during fragmentation. Values for analogous singlets are in brackets.
[c] Data for **S11** re-optimized at the CCSD(T)/CBS//CCSD/aug-cc-pVDZ level.

the diabatic B–C BDHs in the singlets vs. the triplets are more congruous with the expected stronger intrinsic bonding in the singlets and with the larger ρ_b(B–C) values calculated for the singlets (Table 4). The diabatic B–C BDHs in **1** and **5** are also consistent with the diabatic B–C BDH in triplet HBC of 597 kJ/mol.

As both conventional **12**–**15** and unconventional **7**–**9** hydrogen-bonded complexes were located in this study among the more weakly bound triplet isomers (Fig. 1), different types of geometrical rearrangements may be exhibited on complex formation. When an X–H···Y complex containing a conventional hydrogen bond is formed, the X–H bond lengthens typically as a result of electron donation from Y to an antibonding X–H orbital [51]. In an unconventional hydrogen-bonded complex, X is usually a much less electronegative atom, attracting less charge transfer. In this case, the X–H bond may shorten slightly on complex formation [52], which can be explained [51] by the increase in s-character in the X hybrid orbital of the X–H bond dominating the effect of the charge transfer. For purposes of comparison, at the MP2/aug-cc-pVDZ level of theory the bond lengths in H_2, HF and $^3CH_2$ are 0.755, 0.926 and 1.088 Å, respectively.

The strongest FH···Y interactions in isomers **12**–**15** occur when the electron-donating atom in Y is carbon (Table 4). In fact, at 2.2 kJ/mol the $\Delta_{rxn}E$ value for **15** FH···BCH is an order of magnitude smaller than those for **12**–**14**. Among the latter three isomers, the hydrogen bond in **13** FH···CBH, $C_{\infty v}$, with its link through the terminal carbon of HBC is about twice as strong as that in **12** FH···C(B)H, with its link through the medial carbon in HCB. Bending of the linear H···CB angle in **13** to form **14** FH···CBH, C_s weakens the hydrogen bond by only ca.1 kJ/mol. Analysis of the geometrical properties of these four complexes shows that the expected increase in F–H bond length Δr(XH) is observed and that this structural change is directly related to $\Delta_{rxn}E$. The values for Δr(XH) are 0.026 Å (**13** FH···CBH, $C_{\infty v}$) ≈ 0.025 Å (**14** FH···CBH, C_s) > 0.015 Å (**12** FH···C(B)H) > 0.000 Å (**15** FH···BCH). For the three isomers with carbon as the electron-donating atom, $\Delta_{rxn}E$ is inversely related to the H···C distance (Tables 1 and 4).

Comparing **7** HCH···BF and **8** HCH···FB, from the second set of hydrogen-bonded species, it is slightly more favorable for CH_2 to bind through the boron rather than the fluorine. The difference of ~2.5 kJ/mol in the hydrogen-bond strengths of these two complexes is essentially equal to the difference that was observed for the singlet counterparts **S4** HCH···BF and **S5** HCH···FB [1]. For **7** HCH···BF, **8** HCH···FB and **9** HH···BCF, there is essentially no change in the XH bond length on complex formation. Specifically, the values for Δr(XH) are 0.001 Å (**7**) or 0.000 Å (**8** and **9**), indicative of the weak binding and, perhaps, more effective competition between the hyperconjugative and rehybridization effects on formation of these systems (and **15** FH···BCH). The $\Delta_{rxn}E$ values for complexes **7**–**9** and **15** do, however, correlate with the total energy of the hyperconjugative interactions $\Delta E^{(2)}$ (donor → acceptor) and with the bond critical point electron densities in the H···Y bonds ρ_b(H···Y).

For all seven of these hydrogen-bonded complexes $\Delta_{rxn}E$ decreases when $\Delta E^{(2)}$ and ρ_b(H···Y) decrease (Table 4), and the correlation holds across the two sets of isomers despite the variation in both proton-donating and electron-donating atoms. Only the primary contributions to the NBO total hyperconjugation energies will be discussed below. For **13** and **14** the energy ($\Delta E^{(2)}$) contributed by the n(C) → σ*(H–F) hyperconjugation is 203.3 and 181.5 kJ/mol, respectively, whereas for **12** the energy contributed by the σ(C–B) → σ*(H–F) hyperconjugation is 85.2 kJ/mol. Although the magnitudes of these $\Delta E^{(2)}$ values are significantly larger than $\Delta_{rxn}E$ for each of these species (Table 4), because the charge transfer energy is offset by the steric repulsion between the fragments [36], the $\Delta E^{(2)}$ values do account for the relative strengths of the hydrogen bonds in these species. The considerably weaker $\Delta E^{(2)}$ = 14.7 kJ/mol is associated with the n(B) → σ*(H–C) hyperconjugation in **7** HCH···BF. There is an even smaller charge

transfer in **15** FH···BCH from the boron unpaired electron delocalizing into the H–F antibonding orbital, with $\Delta E^{(2)}$ = 5.2 kJ/mol. Weaker still are the $n(F) \rightarrow \sigma^*(H–C)$ and $n(F) \rightarrow \sigma^*(H–H)$ charge transfers in **8** HCH···FB ($\Delta E^{(2)}$ = 3.4 kJ/mol) and **9** HH···FBC ($\Delta E^{(2)}$ = 1.1 kJ/mol), respectively. Consistent with the smaller electron transfer and thus smaller covalent character of the hydrogen bonds in **7**–**9** and **15**, the ρ_b(H···Y) values for these complexes are also an order of magnitude smaller than those for **12**–**14** (Table 4).

As noted earlier, there are four hydrogen-bonded complexes that were located on both the singlet and triplet potential energy surfaces, **7** and **S4** HCH···BF; **8** and **S5** HCH···FB; **12** and **S11** FH···C(B)H; and **13** and **S12** FH···CBH (this work and Ref. [1]). With the exception of **13** and **S12** FH···CBH, the hydrogen bond strengths are essentially identical for the corresponding triplet and singlet complexes. Excitation has enhanced the electron-donating ability of the CBH moiety in **13**, making the hydrogen bond in this complex about 4 kJ/mol stronger than in **S12** (Table 4). Chan et al. saw a similar enhancement in carbonyl oxygen basicity in their comparison of singlet vs. triplet *p*-methoxyacetophenone–H_2O complexes [53].

Finally, isomer **16** can be considered a complex between the fragments H_2BF and C. In this case, the F···C bond has been stretched by ca. 1.1 Å compared to its values in the more tightly bound complexes (Table 1). The flatness and other structural features of the H_2BF fragment indicate that **16** is a complex between ^1H_2BF and ^3C and the associated BDH of 6 kJ/mol reflects the weak interaction resulting from the elongated C···F bond. The NBO analysis [36] gives a total energy of 20 kJ/mol for the hyperconjugative interactions involving only valence-shell orbitals, and the ρ_b(H···Y) value (Table 4) is an order of magnitude smaller than that found for the other C–F bonds (0.23–0.25).

3.2.1.3. Atomization energies and enthalpies of formation. Total atomization energies ΣD_0 were computed for the most stable triplet, **1** H_2CBF, and singlet, **S1** H_2CBF, minima using Eq. (2). The scalar relativistic corrections $\Delta E_{DKH\text{-}SR}$ are small, negative and essentially identical for the singlet (−1.82 kJ/mol) and triplet (−1.73 kJ/mol) species. The spin–orbit correction is $\Delta E_{S\text{-}O}$ = −2.88 kJ/mol for both species. The core–valence corrections ΔE_{CV} are larger, with values of 10.0 kJ/mol for **S1** H_2CBF and 8.0 kJ/mol for **1** H_2CBF. With the scaled C–H stretches, the ΔE_{ZPE} contribution is 73.7 kJ/mol for singlet **S1** and 74.2 kJ/mol for triplet **1**. Combined with the ΔE_{elec}(CBS) values of 1999.6 and 1822.5 kJ/mol for the singlet and triplet, respectively (Table S1), these correction terms lead to total atomization energies of 1931 and 1752 kJ/mol for the singlet and triplet, respectively (Eq. 2). The enthalpies of formation at 0 K derived from these ΣD_0 values are $\Delta_f H$ (^1H_2CBF **S1**) = −145 kJ/mol and $\Delta_f H$ (^3H_2CBF **1**) = 34 kJ/mol, which yield enthalpies of formation at 298 K of $\Delta_f H°_{298}$ (^1H_2CBF **S1**) = −148 kJ/mol and $\Delta_f H°_{298}$ (^3H_2CBF **1**) = 31 kJ/mol. Overall, the differences in the total atomization energies and enthalpies of formation for singlet **S1** H_2CBF and triplet **1** H_2CBF deviate from the differences in the calculated *E* + ZPE values by only 2 kJ/mol (Table 2). We expect the correction terms for the remaining singlet and triplet isomers to be similar in magnitude, indicating that the enthalpies of formation for the remaining isomers can be estimated to ±10 kJ/mol from the relative *E* + ZPE values given in Table 2 and Ref. [1].

3.2.2. Transition structures

The ten identified interconversion pathways between the triplet [B, C, F, H_2] species are depicted in the potential energy diagram in Fig. 4. The barrier heights in the forward and reverse directions, Δ(*E* + ZPE), for the pathways are given in Table 5. The transition structure **TS 2–3** lies ≤3.5 kJ/mol above the reactant

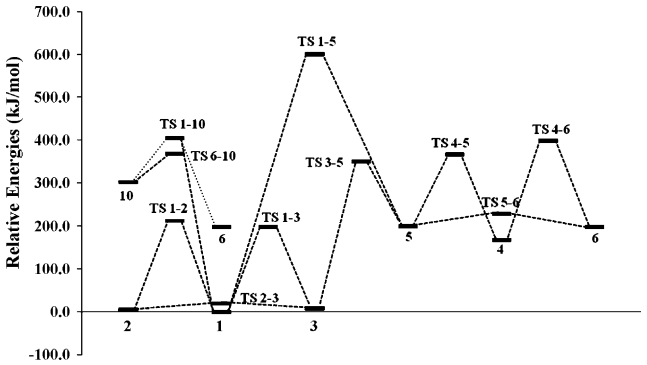

Fig. 4. Reaction profile for the ten identified interconversion pathways. Relative energy data are CCSD(T)/CBS *E* + ZPE values.

Table 5
Transition state barrier heights[a].

Reaction	$\Delta_{rxn}E$	$\Delta_{rxn}(E+ZPE)$
1 $H_2CBF \rightarrow$ **TS 1–2**	226.2	212.5
2 *c*-HCB(F)H → **TS 1–2**	215.5	206.6
1 $H_2CBF \rightarrow$ **TS 1–3**	211.6	198.0
3 *t*-HCB(F)H → **TS 1–3**	198.0	189.1
2 *c*-HCB(F)H → **TS 2–3**	8.0	3.3
3 *t*-HCB(F)H → **TS 2–3**	5.1	0.3
4 $FCBH_2 \rightarrow$ **TS 4–5**	170.0	160.8
5 *t*-H(F)CBH → **TS 4–5**	169.1	155.6
4 $FCBH_2 \rightarrow$ **TS 4–6**	202.3	194.0
6 *c*-H(F)CBH → **TS 4–6**	200.8	188.4
5 *t*-H(F)CBH → **TS 5–6**	32.3	24.1
6 *c*-H(F)CBH → **TS 5–6**	31.7	23.7
1 $H_2CBF \rightarrow$ **TS 1–5**	607.8	591.9
5 *t*-H(F)CBH → **TS 1–5**	411.0	397.5
1 $H_2CBF \rightarrow$ **TS 1–10**	411.1	405.5
10 $BC(H)_2F \rightarrow$ **TS 1–10**	110.1	102.4
3 *t*-HCB(F)H → **TS 3–5**	344.2	338.3
5 *t*-H(F)CBH → **TS 3–5**	161.0	152.8
6 *c*-H(F)CBH → **TS 6–10**	170.3	165.2
10 $BC(H)_2F \rightarrow$ **TS 6–10**	66.8	57.0

[a] CCSD(T)/CBS data in kJ/mol.

2 *c*-HCB(F)H and product **3** *t*-HCB(F)H, implying that there would be essentially free interchange between these isomers and that they would be inseparable or possibly indistinguishable at 298 K. In contrast, the 24 kJ/mol barrier connecting **5** *t*-H(F)CBH and **6** *c*-H(F)CBH suggests that these isomers may be distinguishable and possibly separable at 298 K. Despite the similarity in the stability of **1** H_2CBF compared to **2** and **3** and **4** $FCBH_2$ compared to **5** and **6**, with barrier heights of over 150 kJ/mol these rearrangements are even less likely to be observed at room temperature.

Other than the cis–trans isomerizations the most kinetically viable conversions are **10** → **6** and **10** → **1**, but these conversions still have barriers of more than 55 kJ/mol (Table 5). The H atom displacement (from the four-coordinate carbon atom to the boron) in the first process encounters a barrier about half as high as that of the F atom displacement in the latter process (Fig. 2). Sizable energy barriers also impede the two other processes involving a fluorine atom transfer (**1** ↔ **5** and **3** ↔ **5**), which is not surprising given that bridged fluorine species are uncommon and F radical transfers are less efficient than those of other halogens [54,55]. With respect to the barrier heights, the most noticeable difference in the closed-shell vs. open-shell [B, C, F, H_2] potential energy surfaces is the significantly lower barrier connecting **S1** and **S2**

(53 kJ/mol) than that connecting the analogous **1** and **5** (this work and Ref. [1]).

These results help to explain why it was more difficult to locate transition structures associated with fluorine migrations, and in particular, why we could not locate **TS 1–4**, which would involve exchange of the fluorine and both hydrogens. The remaining interconversions among isomers **2**–**6** and **10** require either a F atom migration or migration of two atoms, and we expect that these processes will pass through transition structures that lie at least as high as those reported in Table 5.

Our results therefore suggest that there are no low-energy barrier pathways separating the other isomers from **1** or from each other, again with exception of the cis–trans isomerizations. As was noted for the singlet PES [1], the barriers are sufficiently high that these species may be experimentally observable at room temperature. In fact, some of these species may be less prone to isomerize than to undergo other reactions.

Acknowledgment

We wish to thank the UMC Division of Information Technology for computer support of the quantum chemical calculations.

Appendix A. Supplementary data

Supplementary data associated with this article can be found, in the online version, at doi:10.1016/j.jfluchem.2009.07.006.

References

[1] C.A. Deakyne, A.K. Corum, H.M. Thomas, F. Liebman, J. Fluorine Chem. 127 (2006) 1355–1367.
[2] F.J. Duncan, R.J. Cvetanovic, J. Am. Chem. Soc. 84 (1962) 3593–3594.
[3] D.V. Lanzisera, L. Andrews, J. Phys. Chem. A 104 (2000) 9295–9301.
[4] R.M. Minyaev, T.N. Gribanova, Russ. J. Gen. Chem. 74 (2004) 1529–1533.
[5] P. Jensen, P.R. Bunker, J. Chem. Phys. 89 (1988) 1327–1332.
[6] M.K. Gilles, K.M. Ervin, J. Ho, W.C. Lineberger, J. Phys. Chem. 96 (1992) 1130–1141.
[7] C.R. Brazier, J. Mol. Spectrosc. 177 (1996) 90–105.
[8] D. Ponomarev, V. Takhistov, S. Slayden, J. Liebman, J. Mol. Struct. 876 (2008) 15–33.
[9] D.J. Grant, D.A. Dixon, J. Phys. Chem. A 113 (2009) 777–787.
[10] D. Feller, K.A. Peterson, D.A. Dixon, J. Chem. Phys. 129 (2008), 204105/1–204105/32.
[11] I. Raabe, D. Himmel, I. Krossing, J. Phys. Chem. A 111 (2007) 13209–13217.
[12] C. Poon, P.M. Mayer, Can. J. Chem. 80 (2002) 25–30.
[13] P.R. Rablen, J.F. Hartwig, J. Am. Chem. Soc. 118 (1996) 4648–4653.
[14] P.R.P. Barreto, A.F.A. Vilela, R. Gargano, Int. J. Quant. Chem. 103 (2005) 659–683.
[15] O. Mó, M. Yáñez, M. Eckart-Maksić, Z.B. Maksić, I. Alkorta, J. Elguero, J. Phys. Chem. A 109 (2005) 4359–4365.
[16] Y. Zeng, K. Su, J. Deng, T. Wang, Q. Zeng, L. Cheng, L. Zhang, THEOCHEM 861 (2008) 103–116.
[17] D.J. Grant, M.H. Matus, J. Switzer, D.A. Dixon, J.S. Francisco, K.O. Christe, J. Phys. Chem. A 112 (2008) 3145–3156.
[18] M.J. Frisch, G.W. Trucks, H.B. Schlegel, G.E. Scuseria, M.A. Robb, J.R. Cheeseman, J.A. Montgomery Jr., T. Vreven, K.N. Kudin, J.C. Burant, J.M. Millam, S.S. Iyengar, J. Tomasi, V. Barone, B. Mennucci, M. Cossi, G. Scalmani, N. Rega, G.A. Petersson, H. Nakatsuji, M. Hada, M. Ehara, K. Toyota, R. Fukuda, J. Hasegawa, M. Ishida, T. Nakajima, Y. Honda, O. Kitao, H. Nakai, M. Klene, X. Li, J.E. Knox, H.P. Hratchian, J.B. Cross, V. Bakken, C. Adamo, J. Jaramillo, R. Gomperts, R.E. Stratmann, O. Yazyev, A.J. Austin, R. Cammi, C. Pomelli, J.W. Ochterski, P.Y. Ayala, K. Morokuma, G.A. Voth, P. Salvador, J.J. Dannenberg, V.G. Zakrzewski, S. Dapprich, A.D. Daniels, M.C. Strain, O. Farkas, D.K. Malick, A.D. Rabuck, K. Raghavachari, J.B. Foresman, J.V. Ortiz, Q. Cui, A.G. Baboul, S. Clifford, J. Cioslowski, B.B. Stefanov, G. Liu, A. Liashenko, P. Piskorz, I. Komaromi, R.L. Martin, D.J. Fox, T. Keith, M.A. Al-Laham, C.Y. Peng, A. Nanayakkara, M. Challacombe, P.M.W. Gill, B. Johnson, W. Chen, M.W. Wong, C. Gonzalez, J.A. Pople, Gaussian 03, Revision C. 02, Gaussian, Inc., Wallingford, CT, 2004.
[19] C. Peng, H.B. Schlegel, Israel J. Chem. 33 (1993) 449–454.
[20] C. Peng, P.Y. Ayala, H.B. Schlegel, M.J. Frisch, J. Comp. Chem. 17 (1996) 49–56.
[21] C. Gonzalez, H.B. Schlegel, J. Chem. Phys. 90 (1989) 2154–2161.
[22] C. Gonzalez, H.B. Schlegel, J. Phys. Chem. 94 (1990) 5523–5527.
[23] C. Gonzalez, H.B. Schlegel, J. Chem. Phys. 95 (1991) 5853–5860.
[24] K.A. Peterson, D.E. Woon, T.H. Dunning Jr., J. Chem. Phys. 100 (1994) 7410–7415.
[25] T.J. Lee, P.R. Taylor, Int. J. Quant. Chem. Quant. Chem. Symp. 23 (1989) 199–207.
[26] M.H. Matus, M.T. Nguyen, D.A. Dixon, K.O. Christe, J. Phys. Chem. A 112 (2008) 4973–4981.
[27] K.A. Peterson, T.H. Dunning Jr., J. Chem. Phys. 117 (2002) 10548–10560.
[28] M. Douglas, N.M. Kroll, Ann. Phys. (NY) 82 (1974) 89–155.
[29] G. Jansen, B.A. Hess, Phys. Rev. A 39 (1989) 6016–6017.
[30] EMSL basis set library, http://www.emsl.pnl.gov/forms/basisform.html.
[31] C.E. Moore, Atomic Energy Levels as Derived from the Analysis of Optical Spectra, vol. 1 H to V, U.S, National Bureau of Standards Circular 467; U.S. Department of Commerce, National Technical Information Service, Washington, DC, 1949, COM-72-50282.
[32] M.W. Chase Jr., J. Phys. Chem. Ref. Data 9 (1998) 1–1951 (NIST-JANAF tables, 4th ed.).
[33] A. Karton, J.M. Martin, J. Phys. Chem. A 111 (2007) 5936–5944.
[34] L.A. Curtiss, K. Raghavachari, P.C. Redfern, J.A. Pople, J. Chem. Phys. 106 (1997) 1063–1079.
[35] E.D. Glendening, A.E. Reed, J.E. Carpenter, F. Weinhold, NBO, Version 3.1., 1993.
[36] A.E. Reed, L.A. Curtiss, F. Weinhold, Chem. Rev. 88 (1988) 899–926.
[37] R.F.W. Bader, Atoms in Molecules. A Quantum Theory, Clarendon Press, Oxford, UK, 1990.
[38] E. Kraka, D. Cremer, in: Z.B. Maksić (Ed.), Theoretical Models of Chemical Bonding. Part 2: The Concepts of the Chemical Bond, Springer, Heidelberg, 1990.
[39] M. Alcamí, O. Mó, M. Yáñez, J.L.M. Abboud, J. Elguero, Chem. Phys. Lett. 172 (1990) 471–477.
[40] G.S. Hammond, J. Am. Chem. Soc. 77 (1955) 334–338.
[41] J.E. Leffler, Science 117 (1953) 340–341.
[42] H.Y. Afeefy, J.F. Liebman, S.E. Stein, in: P.J. Linstrom, W.G. Mallard (Eds.), NIST Chemistry WebBook, NIST Standard Reference Database Number 69, National Institute of Standards and Technology, Gaithersburg, MD, 2009 (retrieved May, 2009) http://webbook.nist.gov.
[43] B.T. Luke, J.A. Pople, M.B. Krogh-Jespersen, Y. Apeloig, M. Karni, J. Chandrasekhar, P.v.R. Schleyer, J. Am. Chem. Soc. 108 (1986) 270–284.
[44] P.v.R. Schleyer, B.T. Luke, J.A. Pople, Organometallics 6 (1987) 1997–2000.
[45] H.A. Bent, Chem. Rev. 61 (1961) 275–311.
[46] A.P. Scott, M.S. Platz, L. Radom, J. Am. Chem. Soc. 123 (2001) 6069–6076.
[47] H. Larsen, K. Hald, J. Olsen, P. Jørgensen, J. Chem. Phys. 115 (2001) 3015–3020.
[48] E.J. Feltham, R.H. Qadiri, E.E.H. Cottrill, P.A. Cook, J.P. Cole, G.G. Balint-Kurti, M.N.R. Ashfold, J. Chem. Phys. 119 (2003) 6017–6031.
[49] A. Pappová, C.A. Deakyne, A. Skancke, I. Cernusák, J.F. Liebman, Mol. Phys. 89 (1996) 247–265.
[50] D. Tzeli, A. Mavridis, J. Phys. Chem. A 105 (2001) 1175–1184.
[51] I.V. Alabugin, M. Manoharan, S. Peabody, F. Weinhold, J. Am. Chem. Soc. 125 (2003) 5973–5987.
[52] P. Hobza, Z. Havlas, Chem. Rev. 100 (2000) 4253–4264.
[53] W.S. Chan, C. Ma, W.M. Kwok, D.L. Phillips, J. Phys. Chem. A 109 (2005) 3454–3469.
[54] J.F. Liebman, B.B. Jarvis, J. Fluorine Chem. 5 (1975) 41–54.
[55] J.F. Liebman, J. Fluorine Chem. 5 (1975) 55–59.